Phosphorus-Containing Dendrimers with Ferrocenyl Units at the Core, within the Branches, and on the Periphery

Cédric-Olivier Turrin, Jérome Chiffre, Dominique de Montauzon, Jean-Claude Daran, Anne-Marie Caminade,* Eric Manoury,* Gilbert Balavoine,* and Jean-Pierre Majoral*

Laboratoire de Chimie de Coordination, CNRS, 205 route de Narbonne 31077 Toulouse Cedex 4, France

Received December 30, 1999; Revised Manuscript Received July 5, 2000

ABSTRACT: The synthesis of new ferrocene derivatives bearing phenoxy and/or formyl groups allows one to obtain phosphorus-containing dendrimers with ferrocene units at the core, within the branches, and at the periphery. Dendrimers with a ferrocene at the core were built from 1,1′-ferrocenedicarboxaldehyde up to the fourth generation. A marked dendritic effect is observed for this family of compounds; indeed, the ferrocenyl core is insulated from the outside in the largest dendrimers (32 or 64 CHO end groups), and the molecule is almost electrochemically inactive. The first dendrimers having three consecutive ferrocene layers within the branches are also described; inner layers are oxidized at the same potential, but the outer layer needs a higher potential to be oxidized, owing to the presence of electron-withdrawing formyl groups. Dendrimers bearing ferrocenyl groups at the periphery are synthesized up to the ninth generation. These compounds are the largest redox active dendrimers ever synthesized; all these ferrocenyl units are oxidized at the same potential, showing that they are all equivalent and electrochemically independent. The exhaustive electrolysis furnishes multiferrocenium dendrimers, which deposit onto electrodes as a stable and conducting film. The multiferrocenium dendrimers can be reduced again quantitatively to neutral dendrimers without apparent decomposition.

Introduction

The chemistry of dendrimers has been developing exponentially for a few years now, due to the unique and fascinating features of these highly branched and well-defined macromolecules.[1] Dendrimers having organometallic centers attract particular attention,[2] and among them, ferrocenyl derivatives of dendrimers appear to possess promising properties.[3] Ferrocenes have often high thermal stability and well-behaved electrochemical properties consisting of a reversible one-electron oxidation, such electron-removal generally not involving a fragmentation of the original skeleton. Furthermore, a large variety of differently substituted ferrocenes can be obtained, often by efficient syntheses, possibly with a controlled planar chirality.[4] So, ferrocenyl derivatives found growing uses in many fields, especially materials chemistry (host−guest chemistry,[5] molecular conductors,[6] molecular materials for nonlinear optics,[7]...) and asymmetric catalysis.[8]

Ferrocenyl moieties have been first linked to the surface of small silicon-containing dendrimers.[9] Such type of compounds can be deposited onto electrode surfaces[10] or used in carbon paste electrodes as mediators in amperometric biosensors for glucose oxidase.[11] Other types of first generation dendrimers possessing ferrocenyl units on the surface have been described;[12] some of them exhibit liquid crystal properties,[13] or possess catalytic activities for asymmetric hydrogenation reactions.[14] Larger ferrocenyl-containing dendrimers have been built, for example, up to the second generation; they possess 16 ferrocenyl units that are either electronically communicated[15] or able to complex cyclodextrin.[16] Dendrimers having 18, 24, or 54 ferrocenyl units are known. Some of them[17] have been found to be suitable to recognize small inorganic anions. A third generation with 24 ferrocenyl units[18] and even a fourth generation dendrimer with 64 ferrocenyl units[19,20] have been described.

In contrast to the grafting of ferrocenyl units onto the surface of dendrimers, which has been studied in several publications, very few papers deal with the presence of ferrocenyl moieties only at the core. A third generation dendron[21] and a fourth generation carbosilane dendrimer were recently reported,[22] the latter having catalytic properties. Dendrimers built with ferrocene derivatives within the branches are unknown; only an organometallic derivative made of 10 ferrocene groups linked to a ferrocene core has been described,[23] but the absence of functional groups on the external Cp prevented the growing of a larger compound. Furthermore, studies of ferrocene-containing dendrimers have been conducted with different types of dendrimers, such as silane dendrimers, poly(propyleneamine) dendrimers, or poly(amide) dendrimers. Thus, it appeared interesting to us to study the influence of the presence of ferrocenyl units at the core, within the branches, and on the surface of a single family of dendrimers.

Some of us have been developing for 6 years the synthesis of phosphorus-containing dendrimers[24] based on the use of 4-hydroxybenzaldehyde and have studied their reactivity at the level of the core,[25] within the branches,[26] and mainly on the surface,[27] including the grafting of organometallic moieties.[28] Therefore, these dendrimers would be suitable to study the influence of the dendritic structure upon ferrocenyl derivatives. For this purpose, we have first prepared new ferrocenyl derivatives, possessing functional groups able to react with the dendritic structure. Then, we have synthesized

* Corresponding authors. Fax: (33) 05 61 55 30 03. E-mail addresses: caminade@lcc-toulouse.fr or manoury@lcc-toulouse.fr or balavoin@lcc-toulouse.fr, or majoral@lcc-toulouse.fr.

10.1021/ma992178f CCC: $19.00
Published on Web 09/06/2000

Scheme 1

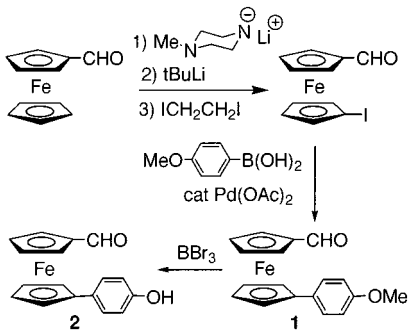

dendrimers with ferrocenyl moieties linked either at the core or within the branches or to the surface and studied their electrochemical properties by cyclic voltammetry and exhaustive electrolysis.

Results and Discussion

Synthesis of the Ferrocenyl Building Blocks. To build up a dendrimer incorporating ferrocenes into the branches, using a procedure derived from the one already reported,[24] we needed a ferrocenyl analogue of 4-hydroxybenzaldehyde. The use of hydroxyferrocenes with the hydroxyl group directly linked to the cyclopentadienyl ring seemed to us to not be very promising because of the instability of this type of compound.[29] On the other hand, ferrocenecarboxaldehydes are quite stable, so we decided to synthesize molecules of type $HOC_6H_4-Z-C_5H_4FeC_5H_4CHO$, Z being a linker between the phenol and the ferrocene. 1,1′-Disubstituted ferrocenes with the same substituents on both cyclopentadienyl groups are easily obtained, owing to the ready synthesis of 1,1′-dilithioferrocene by deprotonation of ferrocene, which leads after quenching with an electrophile to various symmetrically 1,1′-disubstituted ferrocenes.[30] However, we needed an access to dissymmetrically 1,1′-disubstituted ferrocenes to obtain our target molecule.

For this purpose, we decided to try to use 1′-iodoferrocenecarboxaldehyde, which is synthesized from commercially available ferrocenecarboxaldehyde in a one-step procedure.[31] 1′-Iodoferrocenecarboxaldehyde allowed us to obtain the ferrocene derivative **2** in two steps: first, a Suzuki coupling with 4-methoxyphenyl boronic acid[32] yields derivative **1**, and then a deprotection of the methoxy group by BBr_3[33] gives compound **2** (Scheme 1). The overall yield from ferrocenecarbaldehyde is 27%.

Crystals of **1** suitable for X-ray analysis were obtained by slow diffusion of hexane into a dichloromethane solution of **1**. A molecular view (CAMERON)[34] is depicted in Figure 1 with its atom-labeling scheme. Bond distances and angles are in the usual range.[35] The two Cp rings are almost perfectly parallel. The formyl group is roughly in the plane of the adjacent Cp ring with an angle between the two moieties of 4.9°. On the contrary, the phenyl ring is twisted by 16.14° with respect to the Cp ring. Both Cp are nearly staggered with an angle between C(1)−C(11) and C(6)−C(61) vectors of 178.14°.

To graft ferrocenes on the periphery of dendrimers, we needed a ferrocene tethered to a phenol. To facilitate the accommodation of the bulky ferrocene group on the surface of high generation dendrimers, we decided to introduce a CH_2 linker between phenol and ferrocene, to synthesize molecule **6** (Scheme 2). The reaction of

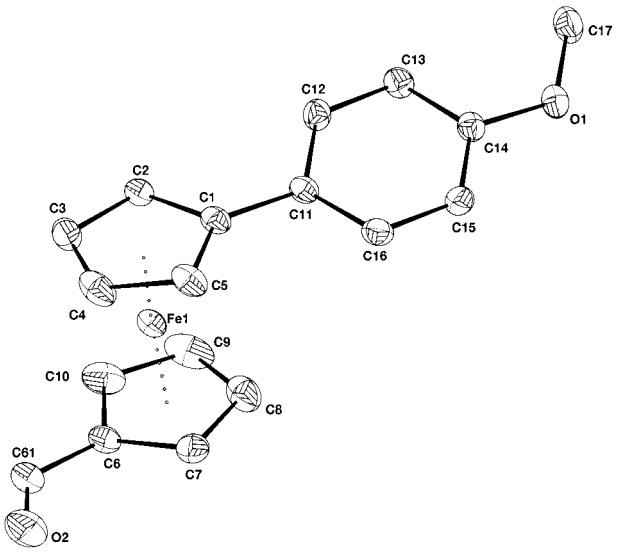

Figure 1. CAMERON drawing of compound **1**.

Scheme 2

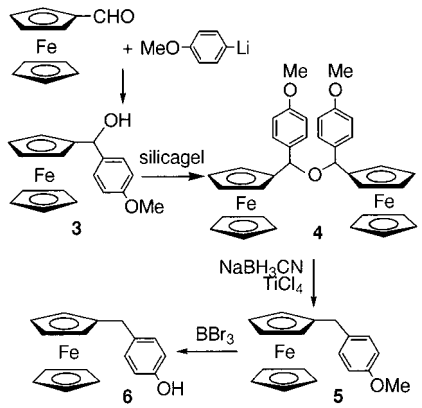

4-methoxyphenyllithium on ferrocenecarboxaldehyde yields quantitatively the alcohol **3**, which dehydrates during the purification on silica gel, giving the ether **4**. The alcohol **3** and the ether **4** are reduced by $NaBH_3CN$, $TiCl_4$ into **5**,[36] which yields the free phenol **6** after deprotection by BBr_3. The overall yield from ferrocenecarboxaldehyde is 68%.

Synthesis of the Dendrimers Incorporating Ferrocenyl Units. To introduce a ferrocene at the core of the dendrimer, we selected 1,1′-ferrocenedicarboxaldehyde **7**, because it will allow the building of one branch on each cyclopentadienyl ring. Furthermore, this compound can be easily obtained by a known procedure from ferrocene.[37] Condensation of the aldehyde groups of **7** with dichloro(methylhydrazino)phosphine sulfide, **8**, leads to compound **7-[G_0]**, then reaction with 4-hydroxybenzaldehyde sodium salt, **9**, gives compound **7-[G'_0]** (Scheme 3). The reiteration of this two steps procedure, i.e., reaction of compounds **7-[G'_n]** (aldehyde end groups) with 2^{n+1} equivalents of **8**, then, substitution of the sodium salt **9** on the $P(S)Cl_2$ groups of dendrimers **7-[G_n]** leads finally to the ferrocenyl dendrimer **7-[G'_4]**, containing 64 CHO end groups. We decided to stop the synthesis at this step, but this compound is not the largest dendrimer obtainable in this series. The structural homogeneity of each generation is checked by size exclusion chromatography, and the completion of reactions is monitored by NMR.[38] The condensation reaction **7-[G'_n]** → **7-[G_{n+1}]** induces the

Scheme 3

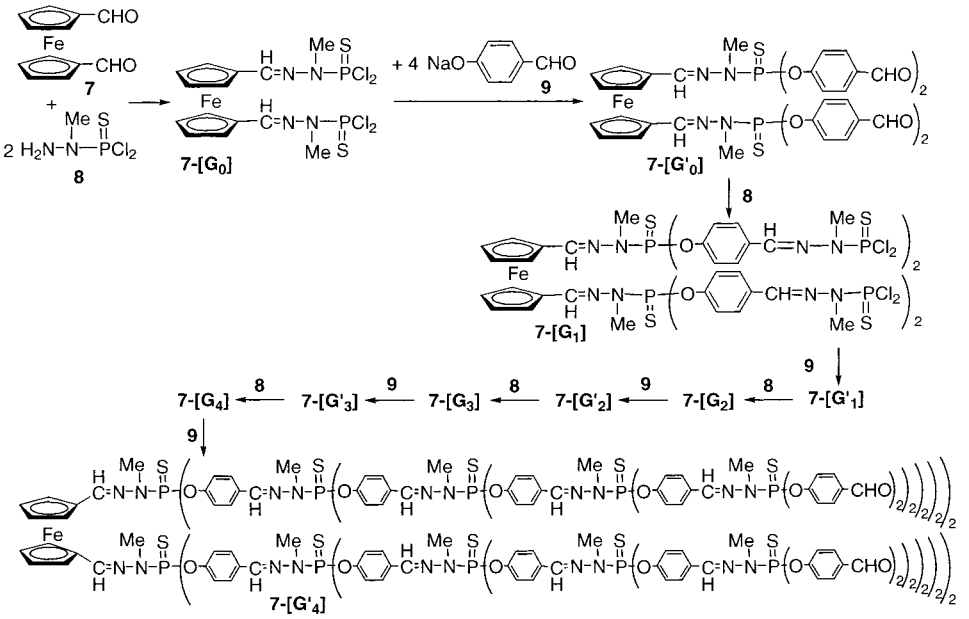

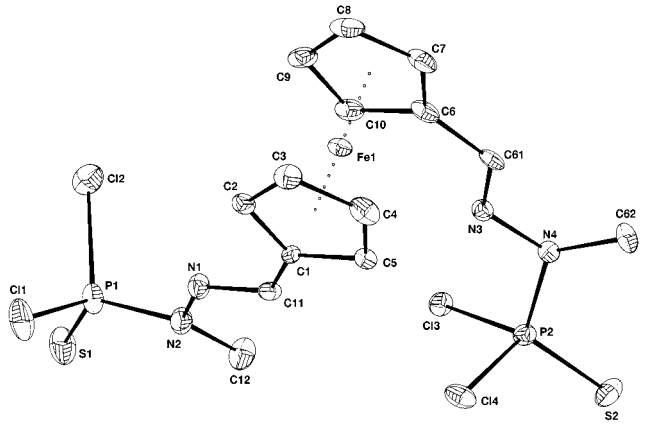

Figure 2. CAMERON drawing of compound **7-[G$_0$]**.

total disappearance of the signals corresponding to the CHO groups in the ^{1}H and ^{13}C NMR spectra as well as in the IR spectra. The transformation **7-[G$_n$]** → **7-[G′$_n$]** induces in ^{31}P NMR the total disappearance of the signal corresponding to the P(S)Cl$_2$ end groups ($\delta \cong 63$ ppm) first on behalf of an intermediate ($\delta \cong 66$ ppm) corresponding to P(S)Cl(OC$_6$H$_4$CHO) end groups, which also disappears to finally give a signal at $\delta \cong 60.5$ ppm corresponding to *P*(*S*)(OC$_6$H$_4$CHO)$_2$ end groups. It can be noticed also that the signals corresponding to the complexed Cp rings are observable in all cases at $\delta \cong$ 4.2 and 4.6 ppm in ^{1}H NMR. Thus, the alternative and repetitive use of the phosphorhydrazide **8** and of the hydroxybenzaldehyde salt **9** allows one to build the dendrimer **7-[G′$_n$]** up to the fourth generation, possessing 64 CHO end groups and a single ferrocenyl group at the core.

Single crystals suitable for X-ray diffraction have been grown for compound **7-[G$_0$]** (two P(S)Cl$_2$ end groups) by slow diffusion of pentane into a solution of **7-[G$_0$]** in CH_2Cl_2. The CAMERON drawing is depicted in Figure 2. Bond distances and bond angles are in the usual range.[24d,26e,27g] The cyclopentadienyl rings and the hydrazone moieties make dihedral angles of 8.03 or 9.68° respectively. It is worth pointing out that each of the hydrazone moieties including the *P*(*S*) group and the carbon linked to the Cp are almost planar, the largest deviation being −0.099 Å at N(2) and 0.150 Å at N(4). Such behavior was already observed for other similar compounds.[24d,26e,27g] The Cp rings are eclipsed, and the relative angle between the C(1)C(11) and C(6)C(61) vectors is 72.72°.

The second series of ferrocenyl-containing dendrimers **11-[G$_n$]** possesses ferrocenyl units within the branches. They are synthesized using the sodium salt **10** of the ferrocenyl derivative **2** as a building block. This difunctionalized organometallic derivative offers a reactivity similar to that of 4-hydroxybenzaldehyde sodium salt **9**: on one hand, the sodium salt of the phenol function allows a nucleophilic substitution on P−Cl bonds; on the other hand, the ferrocenecarboxaldehyde is able to undergo a condensation with the NH_2 group of $Cl_2P(S)N(Me)NH_2$ **8**. Therefore, we decided to reiterate the two steps sequence of reactions previously described, using the ferrocenyl derivative **10** instead of the 4-hydroxybenzaldehyde salt **9**, as shown in Scheme 4. The sequence of reactions was carried out up to the synthesis of dendrimer **11-[G′$_2$]**; however, we had to face some problems concerning the yield of each step. Indeed, we observed in several cases a partial decomposition of the ferrocene moieties, resulting in loss of iron as an insoluble brown powder. Such a destructive phenomenon is presumably due to photodecomposition, known to be quite fast for ferrocenecarboxaldehydes.[39] Several washings allow purifying the dendrimer, but result in a decrease of the yield, which prevented the growing of the dendrimer up to higher generations. The structure of the metallodendrimers **11-[G′$_0$]**−**11-[G′$_2$]** is confirmed by ^{1}H, ^{13}C, and ^{31}P NMR and IR spectroscopies,[38] which give data very close to those already reported for dendrimer **7-G$_n$**. In particular, the disappearance of CHO groups for the **11-[G′$_n$]** → **11-[G$_{n+1}$]** transformation and a shielding effect in ^{31}P NMR spectra for the **11-[G$_n$]** → **11-[G′$_n$]** transformation (from 62.4 to 61.7 ppm) are observed. The ^{13}C NMR spectrum of compound **11-[G′$_2$]** allows to distinguish the three ferrocene layers, in particular with the presence of six singlets corresponding to the quaternary carbon atoms of the Cp rings (81.4 and 87.5 ppm for the first layer Cp$_0$, 81.9 and 87.7

Scheme 4

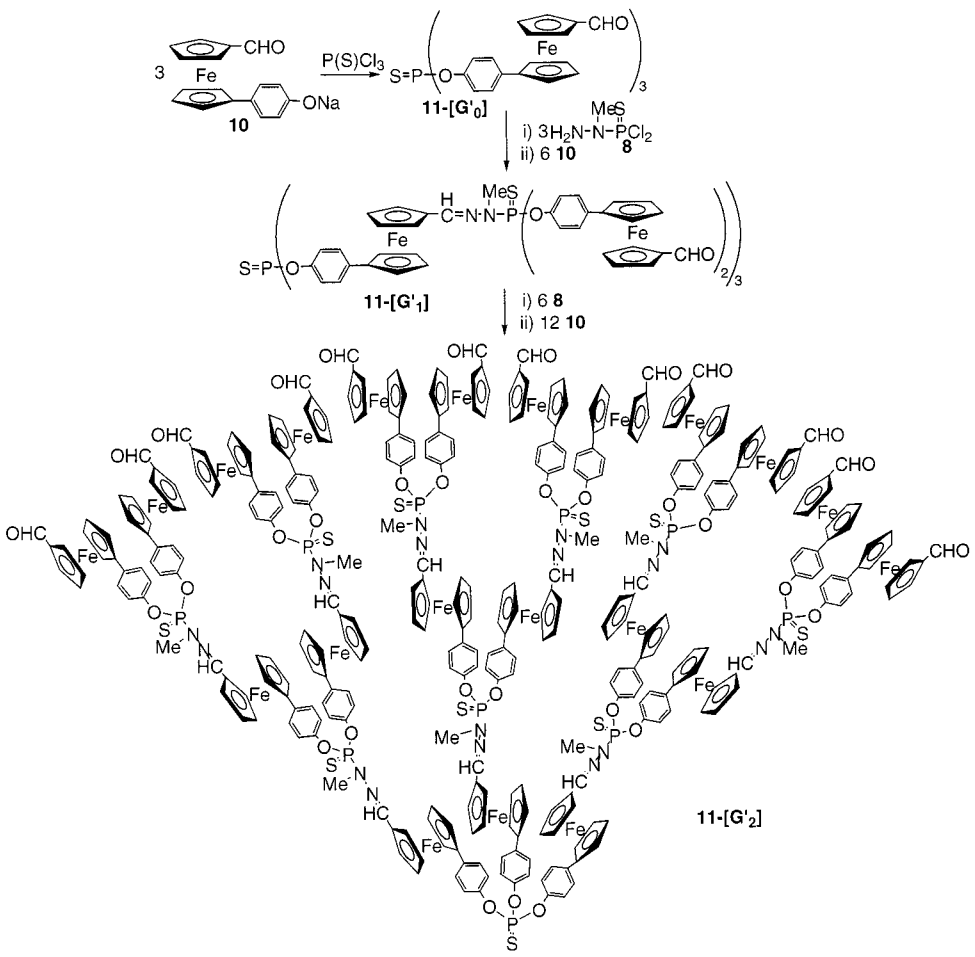

Scheme 5

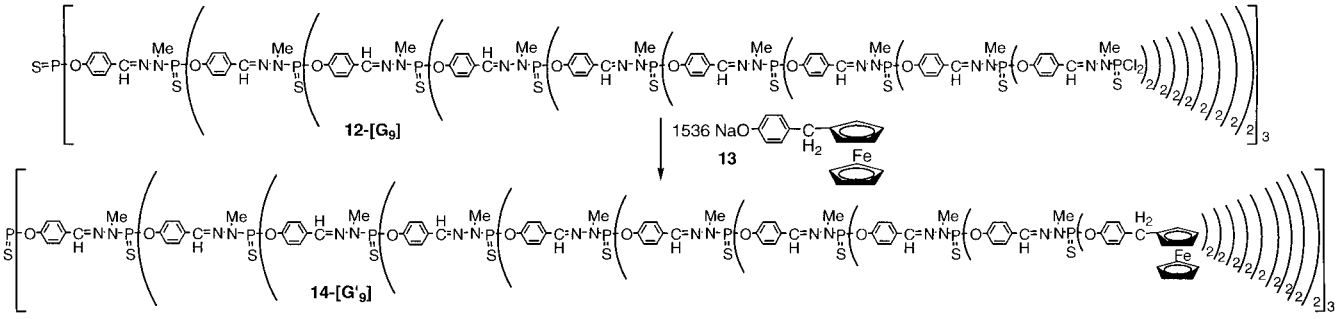

ppm for the second layer Cp_1, and 82.6 and 88.3 ppm for the third layer Cp_2). The efficiency of washings is demonstrated by ^{1}H NMR spectra: no trace of uncomplexed cyclopentadienyl rings is detected in any case. To the best of our knowledge, dendrimer **11-[G′$_2$]** is the largest metallodendrimer incorporating ferrocene units at each layer within the branches and the first one containing iron(II) at three successive layers.

To graft ferrocene derivatives to the surface of dendrimers, we decided to use the nucleophilic substitution of hydroxybenzaldehyde sodium salt derivatives on the $P(S)Cl_2$ end groups of dendrimers built with P(S)O−C_6H_4−CH=N−N(Me)P units. Thus, the third generation dendrimer **12-[G$_3$]**[24] possessing 24 Cl reacts readily with the salt **13**, obtained by reaction of NaH with the ferrocenyl derivative **6** (Scheme 5). The reaction is easily monitored by ^{31}P NMR, which shows the disappearance of the singlet corresponding to the $P(S)Cl_2$ end groups ($\delta = 63.2$ ppm) on behalf of a new singlet at $\delta \cong 63$ ppm, corresponding to the $P(S)[OC_6H_4CH_2FeCp_2]_2$ end groups of **14-[G$_3$]**. The same type of reaction has been applied to the fifth and even to the ninth generation of the dendrimer **12-[G$_n$]**, leading to dendrimers **14-[G$_5$]** and **14-[G$_9$]**, respectively. These compounds are completely characterized by ^{1}H, ^{13}C, and ^{31}P NMR.[38] The structural homogeneity of the samples is checked by SEC, which shows a polydispersity very close to 1 in all cases, as illustrated by the thinness of the SEC traces, even if a small enlargement of the lower part of the signal corresponding to the ninth generation is observed (Figure 3). Compounds **14-[G$_5$]** and **14-[G$_9$]** possess theoretically 96 and 1536 ferrocenyl groups on the periphery, respectively. They are the largest dendritic ferrocenyl derivatives obtained so far.

Electrochemical Studies. Having in hand three series of ferrocene-containing dendrimers, we decided

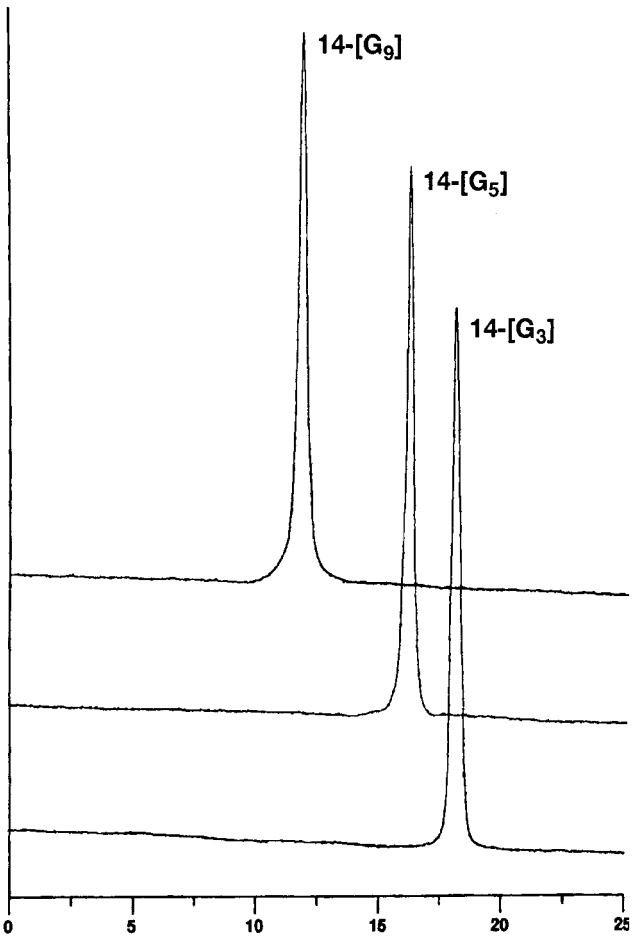

Figure 3. SEC traces of dendrimers **14-[G′3]** **14-[G′5]**, and **14-[G′9]**.

to study their electrochemical behavior, to determine the influence of the position of the ferrocenyl moieties. Their electrochemical parameters were determined in 0.1 M [^{n}Bu$_4$N$^+$][BF$_4^-$] acetone/THF (1:2) solutions (excepted 1:4 for **14-[G9]**) using a conventional three-electrode cell with a Pt working electrode.

Dendrimers Containing FeCp$_2$ Units at the Core. Cyclic voltammetry studies of dendrimers **7-[G′*n*]** provided useful information regarding their redox properties in the solution state (Table 1). The concentration used is 1×10^{-3} mol·L^{-1} for all compounds **7-[G′*n*]**. The cyclic voltammograms of compound **7** and of the lower generation metallodendrimers **7-[G′0]** show characteristic quasi reversible single electron oxidation processes [Fe^{II} → Fe^{III}] (1.09 V for **7** and 0.69 V for **7-[G′0]**) with production of soluble and stable cations (Figure 4). The cathodic shift between **7** and **7-[G′0]** can be explained by changes in the electronic density of the metallic center induced by a weaker electron-withdrawing effect of the hydrazido groups of **7-[G′0]** compared to the aldehyde groups of **7**. These systems exhibit a good electrochemical reversibility ($I_{pc}/I_{pa} \cong 1$ in both cases) and fast electrochemical process ($\Delta E_p = 0.09$ and 0.10 V respectively), as expected for simple ferrocene derivatives.[40] The higher generation dendrimer **7-[G′1]** exhibits a slightly more irreversible process, with $\Delta E_p = 0.12$ V and $I_{pc}/I_{pa} = 0.88$. This trend is confirmed by the pronounced irreversibility of compound **7-[G′2]** (Figure 3). Actually the electroactive core "buried" in the dendritic architecture gives a very weak and poorly resolved signal, with an approximate $\Delta E_p = 0.14$ V. The situation

Table 1. Electrochemical Measurements

compound	e^- [a]	E_{pc} [b]	E_{pa} [b]	$E^{1/2}$ [b]	ΔE_p [c]	I_{pc}/I_{pa}	electrolysis,[d] %
7	1	1.04	1.14	1.09	0.10	1	88
7-G′0	1	0.64	0.73	0.69	0.09	ca. 1	95
7-G′1	1	0.66	0.78	0.72	0.12	0.88	89
7-G′2[e]	1	0.65[f]	0.79[f]	0.72[f]	0.14		*g*
7-G′3[h]	1						
11-G′0	3	0.81	0.90	0.86	0.09	1	85
11-G′1	3	0.65	0.72	0.68	0.07	2	95
	6	0.80	0.86	0.83	0.06	2	*g*
11-G′2	9	0.63	0.70	0.66	0.07	2	110
	12	0.77	0.83	0.80	0.06	1.4	*g*
14-G′3	24	0.50	0.53	0.51	0.03	1.1	96
14-G′5	96	0.48	0.51	0.49	0.03	1.2	98
14-G′9	1536	0.46	0.50	0.48	0.04	1.3	88

[a] Number of electrons theoretically involved. [b] Peak potentials (V vs SCE) at room temperature as determined by cyclic voltammetry at a Pt electrode: $E^{1/2}$ (approximated by $(E_{pc} + E_{pa})/2$) in V vs SCE; supporting electrolyte nBu$_4$N$^+$BF$_4^-$ (0.1 M) in a mixture of THF/acetone (2:1 except for **14-[G′9]** 4:1), scan rate 0.1V·s^{-1}. [c] ($E_{pa} - E_{pc}$) in V. [d] Percentage of FeCp$_2$ sites oxidized in exhaustive coulometry. [e] Poorly resolved signal. [f] Inflection point. [g] Adsorption onto the electrode. [h] No signal.

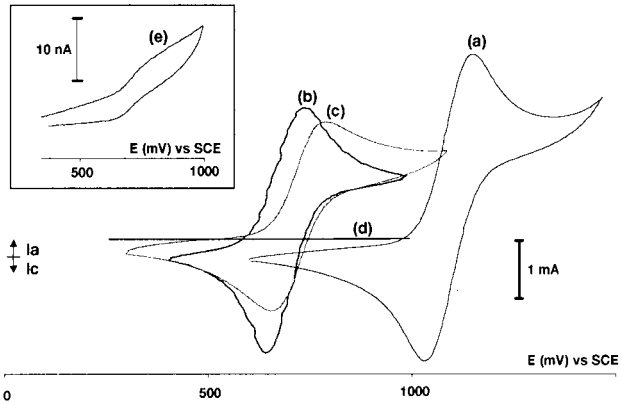

Figure 4. Cyclic voltammograms (scan rate 100 mV·s^{-1}) obtained for compound **7** (a) and dendrimers **7-[G′0]** (b), **7-[G′1]** (c), and **7-[G′2]** (d) and an enlargement for **7-[G′2]** (e). Concentration was 10^{-3} mol·L^{-1} in all cases.

is even worse for dendrimer **7-[G′3]**, which gives a flat current response, the electroactive core being undetectable, with the same concentration as that used for **7-[G′0]** (10^{-3} mol·L^{-1}). These results are in agreement with an analogous behavior, previously reported by several groups working with dendritic architectures containing FeCp$_2$[21] or other electroactive core.[41] As suggested by Kaifer's kinetic electrochemical studies,[21] the electroactive core of dendrimers presenting sufficient steric hindrance cannot approach the electrode close enough, even though the dendritic regions set the minimal distance between the metallic core and the Pt electrode surface, resulting in slow kinetics. Finally, it is worth noting that the $E^{1/2}$ values of our series of dendrimers present a gap from ca. 0.69 to 0.72 V between **7-[G′0]** and higher generation dendrimers. This previously reported behavior[21,41] indicates that the creation of a positive charge in the ferrocene moiety is thermodynamically less favored, in agreement with Creager's results who demonstrated that an increasing hydrophobic environment hinders ferrocene oxidation.[42]

Dendrimers Containing FeCp$_2$ Units within the Branches. The molar concentration in dendrimer used in each case is different, but chosen in order to have a constant concentration in ferrocene units in all cases (5×10^{-3} mol·L^{-1} in iron). The cyclic voltammogram of

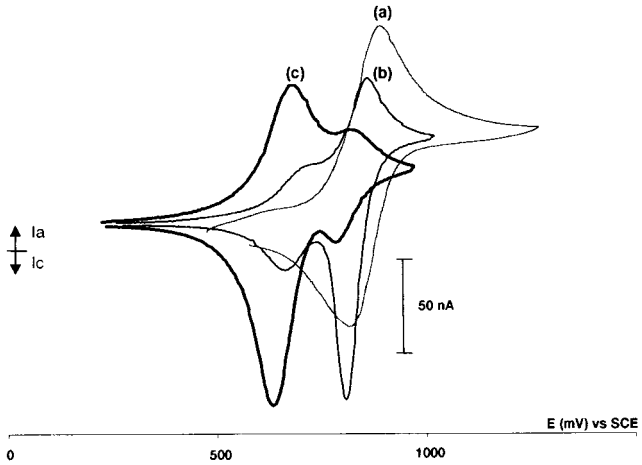

Figure 5. Cyclic voltammograms (scan rate 100 mV·s^{-1}) obtained for dendrimers **11-[G′$_0$]** (a) **11-[G′$_1$]** (b), and **11-[G′$_2$]** (c).

dendrimer **11-[G′$_0$]** shows that the three ferrocenyl moieties, which are reversibly oxidized at 0.86 V ($I_{pc}/I_{pa} = 1$ and $\Delta E_p = 0.09$ V), are equivalent (Table 1, Figure 5). Bulk electrolysis at controlled potential ($E = E^{1/2} + 0.2$ V) confirmed the presence of three equivalent electroactive groups, 85% of the theoretical three electrons per molecule being actually transferred at this potential. Such an experiment affords a stable and soluble tris(ferrocenium) dendrimer.

Dendrimer **11-[G′$_1$]** possessing two layers of ferrocenyl moieties exhibits a first wave at $E^{1/2} = 0.68$ V with a poor resolution, and a second one at $E^{1/2} = 0.83$ V, with a typical well-defined stripping band ($I_{pc}/I_{pa} = 2$) indicating drastic changes in the solubility properties of the oxidation state (Figure 5). The presence of two different waves unambiguously proves that both layers behave independently. The difference between both $E^{1/2}$ values can be correlated to the cathodic shift observed between compounds **7** and **7-[G′$_0$]**. Indeed, the replacement of the aldehyde groups by the hydrazido groups increases the electronic density of the first layer's metallic moieties. Consequently, their potential is shifted from 0.86 V (dendrimer **11-[G′$_0$]**) to 0.68 V (dendrimer **11-[G′$_1$]**), whereas the six electroactive complexes located in the second layer of **11-[G′$_1$]** are oxidized at 0.83 V. Bulk electrolysis at controlled potential allowed to count 3 electrons (with a 95% oxidation ratio) involved in the first transfer: this fact confirms the assignment of this signal to the first layer. Further electrolysis of this dendrimer containing three Fe^{III} and six Fe^{II} moieties was impossible to perform due to deposition upon the Pt working electrode. Nevertheless, we could assign the second wave to the outermost ferrocenes, comparing the current peak intensities measured by square wave voltammetry technique. As shown in Figure 6, the second peak is almost twice higher than the first. The fact that we do not observe a perfect 1/2 ratio for these signals can be explained by a slight overlapping. However, these results appeared reliable enough to assign each wave of the cyclic voltammogram.

Only two signals are also observed when a third layer of ferrocenyl moieties is grafted (**11-[G′$_2$]**) either in cyclic or square wave voltammetry at $E^{1/2} = 0.66$ and 0.80 V (Figure 5). Remarkably, a deep stripping band comes with the well-defined first electronic transfer at $E^{1/2} = 0.66$ V. According to previous results on **7-[G′$_n$]** and **11-[G′$_1$]**, this value is in the range of those observed for

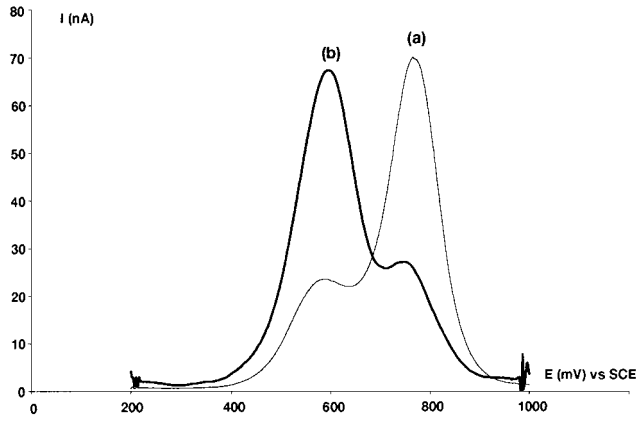

Figure 6. Square wave voltammograms (frequency 50 Hz, potential increment 10 mV) obtained for dendrimers **11-[G′$_1$]** (a) and **11-[G′$_2$]** (b).

hydrazide substituted ferrocenyl moieties. Exhaustive oxidation at 0.70 V allowed counting 10 electrons instead of the 9 electrons expected for both the first and the second layers. This 110% oxidation ratio can be explained by a partial oxidation of the third layer due to poor resolution of the second signal and/or deposition of oxidized products on the Pt gauze electrode. These problems prevented us from carrying out further electrolysis and explain the discrepancy observed in square wave voltammetry between the relative intensity measured for both peaks and the expected 9:12 ratio (Figure 6). It is worth noting that this problem is not due to defects in the end groups of dendrimer **11-[G′$_2$]** which would have been clearly detected in ^{31}P and ^{1}H NMR. Assuming that the 12 outermost ferrocene units of dendrimer **11-[G′$_2$]** behave similarly to the 6 outermost ferrocene units of dendrimers **11-[G′$_1$]**, for which we could obtain reliable and unambiguous electrochemical information, and taking into account the range of $E^{1/2}$ observed for each type of layer (inner/outer) in both compounds, we assigned the second wave at $E^{1/2} = 0.80$ V to the 12 ferrocenyl moieties of the third layer of dendrimer **11-[G′$_2$]**.

Thus, we have demonstrated that the ferrocenyl moieties located within a definite layer of a dendrimer are oxidized at the same potential, with an anodic shift for the potential of the ferrocenyl entities located on the last layer. This difference observed between inner and outer layers can be explained in the light of electronic effects exerted by the electron-withdrawing aldehyde group for the outer ferrocenes, in comparison with that exerted by the hydrazido group for the inner ones.

Dendrimers Containing $FeCp_2$ Units on the Periphery. Dendrimers **14-[G′$_3$]** **14-[G′$_5$]** and **14-[G′$_9$]** were all studied in the same mixture of solvents (acetone/THF), but **14-[G′$_9$]** required a higher proportion of THF to be solubilized. In this case also, the concentration in ferrocene units is kept constant (2.5×10^{-3} mol·L^{-1}), but of course the molar concentration in dendrimer is different for each generation. Dendrimers **14-[G′$_3$]** to **14-[G′$_9$]** exhibit a single oxidation wave at ca. 500 mV corresponding to a multielectronic transfer of the equivalent and electrochemically independent ferrocenyl end groups. This independent behavior of the outer metal complexes was first reported by Cuadrado et al.[10] for silicon-containing dendrimers from generation 1 to 4.[19,20] The fact that it is still observed for the ninth generation **14-[G′$_9$]** (Figure 7) confirms the absence of steric hindrance for this family of phosphorus-

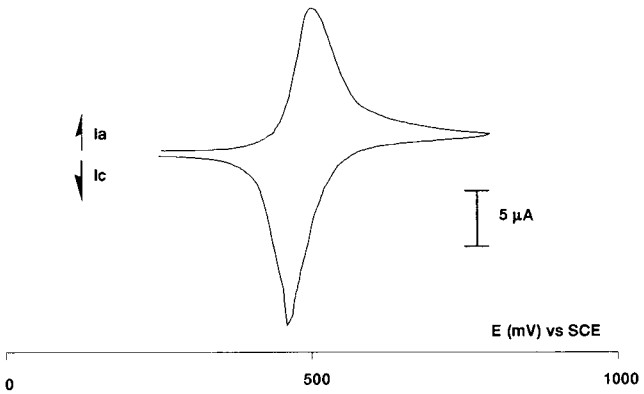

Figure 7. Typical cyclic voltammogram (scan rate 100 $mV \cdot s^{-1}$) obtained for dendrimer **14-[G′9]**.

containing dendrimers, even for very high generations.[27g] The reduction wave presents a typical stripping shape, indicating that the redox behavior of this series of compounds is marked by changes in solubility properties in the oxidation state. Actually, the multiferrocenium obtained upon exhaustive electrolysis at controlled potential ($E = E^{1/2} + 0.2$ V) deposits onto the Pt gauze electrode surface to form a blue conducting film. Reduction of the film induces its total desorption and allows recovering the neutral starting dendrimers without chemical modification discernible in NMR spectra. As expected, the theoretical number of transferred electrons is never completed, however, 88−98% of the $FeCp_2$ sites are oxidized (23/24 for **14-[G′3]**, 94/96 for **14-[G′5]**, and 1352/1536 for **14-[G′9]**). It must be emphasized that this observation must not be systematically correlated to defects on the surface; even very simple monoferrocenyl derivatives give less than 100% charge recovery (see for instance 88% for **7**). Furthermore, the adsorption onto the electrode observed for most dendrimers can also modify the measurement of transferred electrons. Anyway, the 1352 electrons actually counted for **14-[G′9]** are by far the largest number of electrons measured up to now by electrochemistry for any type of dendrimer.

Conclusion

The obtaining of new ferrocenyl derivatives having phenoxy and/or aldehyde functions linked to the Cp rings led to the synthesis of three families of dendrimers, possessing ferrocene derivatives either at the core (**7-[G0]**−**7-[G′4]**), within the branches (**11-[G′0]**−**11-[G′2]**), or at the surface (**14-[G′3], 14-[G′5], 14-[G′9]**), and all based on the use of $P(S)OC_6H_4ZCH{=}NN(Me)P$ linkages (Z = nothing for **7-[G′n]** and **14-[G′n]**, Z = ferrocene for **11-[G′n]**). The close relationship between the three families allows for the first time to effect a global study concerning the influence of the localization of electroactive entities upon their properties.

The presence of a single ferrocenyl group at the core of compounds **7-[G′n]** allows to observe a marked dendritic effect; important differences are noted between the electrochemical properties of compounds **7-[G′1]** (eight CHO end groups) and **7-[G′2]** (16 CHO end groups). The former compound shows a quasi-reversible oxidation process, whereas the latter shows a pronounced irreversibility and a very weak signal at the same concentration. This behavior indicates that the dendritic superstructure is rapidly able to "bury" the electroactive core, as confirmed by the flat current response given by dendrimer **7-[G′3]** (32 CHO end groups).

Compound **11-[G′2]** is the first example of a dendrimer possessing ferrocenyl derivatives at three layers within the branches. In contrast to NMR experiments which allows distinguishing the three layers, electrochemistry only distinguishes the inner and the outer layers. Both inner layers are oxidized at the same potential, and more easily than the outer layer, indicating that electronic effects have a greater importance than the localization upon the oxidation process. Surprisingly, oxidation of the inner layers induces drastic changes in the solubility of dendrimers. This behavior is in marked contrast with most previous observations, indicating that the solubility is mainly governed by the functions located on the surface.

Ferrocene derivatives linked to the surface of dendrimers exhibit a single oxidation wave, indicating that all of them behave independently, even for the very large ninth generation dendrimer **14-[G′9]**. This fact confirms the absence of steric hindrance for the high generations of this family of phosphorus-containing dendrimers. Compounds **14-[G′5]** and above all compound **14-[G′9]** are the largest redox active dendrimers ever synthesized. The multiferrocenium derivatives obtained from their exhaustive electrolysis deposit onto the Pt electrode surface to form conducting films, stable at least for several days to air and moisture. Such behavior leads to the formation of modified electrodes, which may serve as multielectron catalysts, multielectron reservoirs, or chemical sensors.

Experimental Section

General Data. All reactions were carried out in the absence of air using standard Schlenk techniques and vacuum-line manipulations and with protection against light. All solvents were dried and distilled before use. Thin-layer chromatography was carried out on Merck Kieselgel $60F_{254}$ precoated silica gel plates. Preparative flash chromatography was performed on Merck Kieselgel. Instrumentation: Bruker AC80, AC200, AM250, DPX 300 (^1H, ^{13}C, ^{31}P NMR); Perkin-Elmer 1725X (FT-IR). Elemental analyses were performed by the Service d'Analyse du Laboratoire de Chimie de Coordination, Toulouse, France. Size Exclusion Chromatography analytical data were obtained using a Waters 410 differential diffractometer at 37 °C, with three 5 μm Waters Styragel HR columns connected in series in order of decreasing pore size (10000, 1000, and 100 Å) and THF as eluent with a nominal flow of 1.2 $mL \cdot min^{-1}$. 1,1′-Ferrocenedicarboxaldehyde,[35] dichlorothiophosphorhydrazide (**8**),[24] and dendrimers **12-[Gn]**[24] were prepared according to published procedures.

Electrochemical Measurements. Voltammetric and electrolytic measurements were carried out with a homemade potentiostat[43] using the interrupt method to minimize the uncompensated resistance (Ri) drop; square wave voltammetry measurements were carried out on a PAR model 273. Experiments were performed at room temperature in an airtight three-electrode cell connected to a vacuum/argon line. The reference electrode consisted of a saturated calomel electrode (SCE) separated from the solutions by a bridge compartment. The counter electrode was a spiral of ca. 1 cm^2 apparent surface, made of a platinum wire 8 cm in length and 0.5 cm in diameter. The working electrode was a Pt electrode (1 mm diameter) for cycling voltammetry and a Pt gauze electrode for bulk electrolysis. $E^{1/2}$ values were determined as the average of the cathodic and the anodic peak potentials. The supporting electrolyte (nBu$_4$N)[BF_4] (Fluka, electrochemical grade) was used as received.

X-ray Crystal Structure Determination. Crystals suitable for X-ray analysis were obtained by slow diffusion of hexane or pentane into a dichloromethane solution of the studied compound. For **1** and **7-[G0]**, data were collected on a STOE IPDS diffractometer equipped with a graphite oriented

Table 2. Crystal Data

	1	**7-[G$_0$]**
formula	$C_{18}H_{16}O_2Fe$	$C_{14}H_{16}N_4P_2S_2Cl_2Fe$
fw, g	320.17	564.0(2)
shape (color)	flat box (dark red)	flat (colorless)
size, mm	0.32, 0.27, 0.13	
space group	$P2_1/c$	$P2_1/c$
a, Å	14.432(2)	10.324(2)
b, Å	7.4363(8)	7.3451(7)
c, Å	13.172(2)	29.871(4)
β, °	90.64(2)	93.60(2)
V, Å^3	1413.1(5)	2260.7(5)
Z	4	
temp, K	293(2)	140(2)
R	0.0270	0.1021
R_w	0.0325	0.0583
GOF	1.004	1.0359

monochromator utilizing Mo Kα radiation (λ = 0.710 73) at room temperature for **1** and at 140 K for **7-[G$_0$]**. The final unit cell parameters were obtained by the least-squares refinement of 5000 reflections. Only statistical fluctuations were observed in the intensity monitors over the course of the data collections.

The two structures were solved by direct methods (SIR92[44]) and refined by least-squares procedures on F. All H atoms attached to carbon were introduced in calculation in idealized positions (d(CH) = 0.96 Å) and their atomic coordinates were recalculated after each cycle. They were given isotropic thermal parameters 20% higher than those of the carbon to which they are attached. Least-squares refinements were carried out by minimizing the function $\sum w(|F_o| - |F_c|)^2$, where F_o and F_c are the observed and calculated structure factors. The weighting scheme used in the last refinement cycles was $w = w'[1-\{\Delta F/6\sigma(F_o)\}^2]^2$ where $w' = 1/\sum_1^n A_r T_r(x)$ with three coefficients A_r for the Chebyshev polynomial $A_r T_r(x)$ where x was F_c/F_c(max).[45] Models reached convergence with $R = \sum(||F_o| - |F_c||)/\sum(|F_o|)$ and $R_w = [\sum_w(|F_o| - |F_c|)^2/\sum w(F_o)^2]^{1/2}$, having values listed in Table 2. Crystals obtained for **7-[G$_0$]** were poorly crystallized and led to a set of data of rather poor quality with a high merging factor of 0.126. No better quality crystals could be obtained, but although the structural analysis of **7-[G$_0$]** is not of a high standard, there is no doubt of the reality of the structure.

The calculations were carried out with the CRYSTALS package programs[46] running on a PC. Full crystal data, fractional atomic coordinates, anisotropic thermal parameters for non-hydrogen atoms, atomic coordinates for H atoms, and a full list of bond lengths and bond angles have been deposited at the Cambridge Crystallographic Data Center.

Acknowledgment. Thanks are due to the CNRS for financial support, to DGA (France) for a grant to C.-O. T., and to M. Mauzac for SEC experiments.

Supporting Information Available: Text giving the method of synthesis and characterization (^{1}H, ^{13}C, ^{31}P NMR, IR, elemental analyses) of all new compounds (24 compounds), figures showing the numbering scheme used for NMR data, SEC traces of compounds **7-[G′$_0$]**−**7-[G′$_4$]** and the structure of compound **14-[G′$_5$]**, and tables of crystal data, interatomic distances and angles, atomic coordinates, and isotropic and anisotropic parameters. This material is available free of charge via the Internet at http://pubs.acs.org.

References and Notes

(1) For reviews concerning dendrimers see for example: (a) Tomalia, D. A.; Naylor, A. M.; Goddard, W. A., III. *Angew. Chem., Int. Ed. Engl.* **1990**, *29*, 138. (b) Issberner, J.; Moors, R.; Vögtle, F. *Angew. Chem., Int. Ed. Engl.* **1994**, *33*, 2413. (c) Ardoin, N.; Astruc, D. *Bull. Soc. Chim. Fr.* **1995**, *132*, 876. (d) Newkome, G. R.; Moorefield, C. N.; Vögtle, F. In *Dendritic Molecules*, VCH: Weinheim, Germany, 1996. (e) Gudat, D. *Angew. Chem., Int. Ed. Engl.* **1997**, *36*, 1951. (f) Majoral, J. P.; Caminade, A. M. *Top. Curr. Chem.* **1998**, *197*, 79. (g) Chow, H. F.; Mong, T. K. K.; Nongrum, M. F.; Wan, C. W. *Tetrahedron* **1998**, *54*, 8543. (h) Majoral, J. P.; Caminade, A. M. *Chem. Rev.* **1999**, *99*, 845.

(2) See for example: (a) Gorman, C. *Adv. Mater.* **1998**, *10*, 295. (b) Venturi, M.; Credi, A.; Balzani, V. *Coord. Chem. Rev.* **1999**, *185*−*186*, 233. (c) Newkome, G. R.; He, E.; Moorefield, C. N. *Chem. Rev.* **1999**, *99*, 1689.

(3) (a) Cuadrado, I.; Morán, M.; Losada, J.; Casado, C. M.; Pascual, C.; Alonso, B.; Lobete, F. In *Advances in Dendritic Macromolecules*; Newkome G. R., Ed.; JAI: Greenwich, CT, 1996, Vol. 3, p 151. (b) Casado, C. M.; Cuadrado, I.; Morán, M.; Alonso, B.; Garcia, B.; González, B.; Losada, J. *Coord. Chem. Rev.* **1999**, *185*−*186*, 53.

(4) (a) Richards, C. J.; Locke, A. J. *Tetrahedron Asym.* **1998**, *9*, 2377. (b) Balavoine, G. G. A.; Daran, J.-C.; Iftime, G.; Manoury, E.; Moreau-Bossuet, C. *J. Organomet. Chem.* **1998**, *567*, 191. (c) Wagner, G.; Herrmann, R. In *Ferrocenes*, Togni, A., Hayashi, T., Eds.; VCH: Weinheim, Germany, 1995; pp 173−214.

(5) Togni, A. In *Ferrocenes*, Togni, A., Hayashi, T., Eds.; VCH: Weinheim, Germany, 1995; pp 433−466.

(6) (a) Beer, P. D. *Acc. Chem. Res.* **1998**, *31*, 71. (b) van Veggel, F. C. J. M.; Verboom, W.; Reinhoudt, D. N. *Chem. Rev.* **1994**, *94*, 279.

(7) (a) Whittall, I. R.; McDonagh, A. M.; Humphrey, M. G. *Adv. Organomet. Chem.* **1998**, *42*, 291. (b) Long, N. J. *Angew. Chem., Int. Ed. Engl.* **1995**, *34*, 21. (c) Marder, S. R. In *Inorganic Materials*; Bruce, D. W., O'Hare, D., Eds.; John Wiley & Sons: New York, 1992, pp 115−164.

(8) Hayashi, T. In *Ferrocenes*, Togni, A., Hayashi, T., Eds.; VCH: Weinheim, Germany, 1995; pp 105−139.

(9) Alonso, B.; Cuadrado, I.; Morán, M.; Losada, J. *J. Chem. Soc., Chem. Commun.* **1994**, 2575.

(10) (a) Alonso, B.; Morán, M.; Casado, C. M.; Lobete, F.; Losada, J.; Cuadrado, I. *Chem. Mater.* **1995**, *7*, 1440. (b) Casado, C. M.; Cuadrado, I.; Morán, M.; Alonso, B.; Garcia, B.; Gonzalez, B.; Losada, J. *Coord. Chem. Rev.* **1999**, *185*−*186*, 53.

(11) Losada, J.; Cuadrado, I.; Morán, M.; Casado, C. M.; Alonso, B.; Barranco, M. *Anal. Chim. Acta* **1997**, *338*, 191.

(12) Achar, S.; Immoos, C. E.; Hill, M. G.; Catalano, V. J. *Inorg. Chem.* **1997**, *36*, 2314.

(13) Deschenaux, R.; Serrano, E.; Levelut, A. M. *Chem. Commun.* **1997**, 1577.

(14) Köllner, C.; Pugin, B.; Togni, A. *J. Am. Chem. Soc.* **1998**, *120*, 10274.

(15) Cuadrado, I.; Casado, C.; Alonso, B.; Morán, M.; Losada, J.; Belsky, V. *J. Am. Chem. Soc.* **1997**, *119*, 7613.

(16) Castro, R.; Cuadrado, I.; Alonso, B.; Casado, C. M.; Morán, M.; Kaifer, A. E. *J. Am. Chem. Soc.* **1997**, *119*, 5760.

(17) (a) Valério, C.; Fillaut, J. L.; Ruiz, J.; Guittard, J.; Blais, J. C.; Astruc, D.*J. Am. Chem. Soc.* **1997**, *119*, 2588. (b) Guittard, J.; Blais, J. C.; Astruc, D.; Valério, C.; Alonso, E.; Ruiz, J.; Fillaut, J. L. *Pure Appl. Chem.* **1998**, *70*, 809. (c) Valério, C.; Alonso, E.; Ruiz, J.; Blais, J. C.; Astruc, D. *Angew. Chem., Int. Ed. Engl.* **1999**, *38*, 1747. (d) Nlate, S.; Ruiz, J.; Blais, J. C.; Astruc, D. *Chem. Commun.* **2000**, 417.

(18) Shu, C. F.; Shen, H. M. *J. Chem. Mater.* **1997**, *7*, 47.

(19) Cuadrado, I.; Morán, M.; Casado, C. M.; Alonso, B.; Lobete, F.; García, B.; Ibisate, M.; Losada, J. *Organometallics* **1996**, *15*, 5278.

(20) Takada, K.; Díaz, D. J.; Abruña, H. D.; Cuadrado, I.; Casado, C.; Alonso, B.; Morán, M.; Losada, J. *J. Am. Chem. Soc.* **1997**, *119*, 10763.

(21) (a) Cardona, C. M.; Kaifer, A. E. *J. Am. Chem. Soc.* **1998**, *120*, 4023. (b) Kaifer, A. E. *Acc. Chem. Res.* **1999**, *32*, 62. (c) Wang, Y.; Cardona, C. M.; Kaifer, A. E. *J. Am. Chem. Soc.* **1999**, *121*, 9756. (d) Cardona, C. M.; McCarley, T. D.; Kaifer, A. E. *J. Org. Chem.* **2000**, *65*, 1857.

(22) Oosterom, G. E.; van Haaren, R. J.; Reek, J. N. H.; Kamer, P. C. J.; van Leewen, P. W. N. M. *Chem. Commun.* **1999**, 1119.

(23) Jutzi, P.; Batz, C.; Neumann, B.; Stammler, H. G. *Angew. Chem., Int. Ed. Engl.* **1996**, *35*, 2118.

(24) (a) Launay, N.; Caminade, A.-M.; Lahana, R.; Majoral, J.-P. *Angew. Chem., Int. Ed. Engl.* **1994**, *33*, 1589. (b) Launay, N.; Caminade, A.-M.; Majoral, J.-P. *J. Am. Chem. Soc.* **1995**, *117*, 3282. (c) Galliot, C.; Prévôté, D.; Caminade, A. M.; Majoral, J. P. *J. Am. Chem. Soc.* **1995**, *117*, 5470. (d) Lartigue, M. L.; Launay, N.; Donnadieu, B.; Caminade, A. M.; Majoral, J. P. *Bull. Soc. Chim. Fr.* **1997**, *134*, 981.

(25) Maraval, V.; Laurent, R.; Donnadieu, B.; Mauzac, M.; Caminade A. M.; Majoral, J. P. *J. Am. Chem. Soc.* **2000**, *122*, 2499.
(26) (a) Galliot, C.; Larré, C.; Caminade, A. M.; Majoral, J. P. *Science* **1997**, *277*, 1981. (b) Larré, C.; Caminade, A. M.; Majoral, J. P. *Angew. Chem., Int. Ed. Engl.* **1997**, *36*, 596. (c) C. Larré, C.; Donnadieu, B.; Caminade, A. M.; Majoral, J. P. *Chem. Eur. J.* **1998**, *4*, 2031. (d) Larré, C.; Donnadieu, B.; Caminade, A. M.; Majoral, J. P. *J. Am. Chem. Soc.* **1998**, *120*, 4029. (e) Larré, C.; Bressolles, D.; Turrin, C.; Donnadieu, B.; Caminade, A. M.; Majoral, J. P. *J. Am. Chem. Soc.* **1998**, *120*, 13070.
(27) (a) Launay, N.; Slany, M.; Caminade, A.-M.; Majoral, J.-P. *J. Org. Chem.* **1996**, *61*, 3799. (b) Lartigue, M.-L.; Slany, M.; Caminade, A.-M.; Majoral, J.-P. *Chem.—Eur. J.* **1996**, *2*, 1417. (c) Slany, M.; Caminade, A.-M.; Majoral, J.-P. *Tetrahedron Lett.* **1996**, *37*, 9053. (d) Prévôté, D. Caminade, A.-M.; Majoral, J.-P. *J. Org. Chem.* **1997**, *62*, 4834. (e) Lartigue, M.-L.; Caminade, A.-M.; Majoral, J.-P. *Tetrahedron Asym.* **1997**, *8*, 2697. (f) Prévôté, D.; Le Roy-Gourvenec, S.; Caminade, A.-M.; Masson, S.; Majoral, J.-P. *Synthesis* **1997**, 1199. (g) Lartigue, M.-L.; Donnadieu, B.; Galliot, C.; Caminade, A.-M.; Majoral, J.-P.; Fayet, J.-P. *Macromolecules* **1997**, *30*, 7335.
(28) (a) Slany, M.; Bardaji, M.; Casanove, M. J.; Caminade, A.-M.; Majoral, J.-P.; Chaudret, B. *J. Am. Chem. Soc.* **1995**, *117*, 9764. (b) Bardaji, M.; Kustos, M.; Caminade, A.-M.; Majoral, J.-P.; Chaudret, B. *Organometallics* **1997**, *16*, 403. (c) Slany M.; Bardaji, M.; Caminade, A.-M.; Chaudret, B.; Majoral, J.-P. *Inorg. Chem.* **1997**, *36*, 1939. (d) Bardaji, M.; Caminade, A.-M.; Majoral, J.-P.; Chaudret B.*Organometallics* **1997**, *16*, 3489. (e) Caminade, A. M.; Laurent, R.; Chaudret, B.; Majoral, J. P. *Coord. Chem. Rev.* **1998**, *178*, 793.
(29) Herberhold, M. In *Ferrocenes*; Togni, A., Hayashi, T., Eds.; VCH: Weinheim, Germany, 1995; pp 229−230.
(30) Butler, I.; Cullen, W. R.; Ni, J.; Rettig, S. J. *Organometallics* **1985**, *4*, 2196.
(31) Iftime, G.; Moreau-Bossuet, C.; Manoury, E.; Balavoine, G. G. A. *J. Chem. Soc., Chem. Commun.* **1996**, 527.
(32) Brunner, A.; Taudien, S.; Riant, O.; Kagan, H. B. *Chirality* **1997**, *9*, 478.
(33) Vickery, E. H.; Pahler, L. F.; Eisenbraun, E. J. *J. Org. Chem.* **1979**, *44*, 4444.
(34) Watkins, D. J.; Prout, C. K.; Pearce, L. J. CAMERON. Chemical Crystallography Laboratory, University of Oxford: Oxford, England, 1996.
(35) (a) Gallagher, J. F.; Ferguson, G.; Ahmed, S. Z.; Glidewell, C.; Lewis, A. *Acta Crystallogr., Sect. C (Cryst. Struct. Commun.)* **1997**, *53*, 1772. (b) Wong, W.-Y.; Wong, W.-T. *J. Chem. Soc., Dalton Trans.* **1996**, 3209.
(36) Bhattacharyya, S. *Synlett* **1995**, 971.
(37) Balavoine, G. G. A.; Doisneau, G.; Fillebeen-Khan, T. *J. Organomet. Chem.* **1991**, *412*, 381.
(38) The molecular peak of these phosphorus-containing dendrimers is detected by MALDI−TOF experiments in several cases. However, this technique is not reliable to detect structure defects since the UV spectra of these dendrimers show a very broad absorption at 210−360 nm, i.e. including the wavelength of the MALDI−TOF laser (337 nm); thus, the laser irradiation provokes the cleavage of a number of bonds (hydrazone units), which induces the appearance of a large number of new peaks in ^{31}P and ^{1}H NMR. Furthermore, a dramatic broadening of the SEC trace (the width of the line at half-maximum intensity is multiplied by more than 10 after irradiation) is also observed: Blais, J. C.; Turrin, C. O.; Caminade, A. M.; Majoral, J. P. *Anal. Chem.*, in press.
(39) Davis, J.; Vaughan, D. H.; Cardosi, M. F.; *Electroanalysis* **1999**, *9*, 650.
(40) Kaifer, A. E. In *Transition Metal in Supramolecular Chemistry*; Fabbrizzi, L., Poggi, A., Eds.; NATO ASI Series; Kluwer: Dordrecht, The Netherlands, 1994; p 227.
(41) Smith, D. K.; Diederich, F. *Chem.—Eur. J.* **1998**, *4*, 1353.
(42) Rowe, G. K.; Creager, S. E. *Langmuir* **1991**, *7*, 2307.
(43) Cassoux, P.; Dartiguepeyron, R.; de Montauzon, D.; Tommasino, J. B.; Fabre, P. L. *Actual. Chim.* **1994**, *1*, 49.
(44) Altomare, A.; Burla, M. C.; Camalli, M.; Cascarano, G.; Giacovazzo, C.; Guagliardi, A.; Polidori, G. *J. Appl. Crystallogr.* **1994**, *27*, 435.
(45) Prince, E. *Mathematical Techniques in Crystallography*; Springer-Verlag: Berlin, 1982.
(46) Watkin, D. J.; Prout, C. K.; Carruthers, J. R.; Betteridge, P. W. *CRYSTALS Issue 10*; Chemical Crystallography Laboratory, University of Oxford: Oxford, England, 1996.

MA992178F